Bull. Chem. Soc. Ethiop. **2025**, 39(7), 1395-1410.
DOI: https://dx.doi.org/10.4314/bcse.v39i7.12

ISSN 1011-3924
Printed in Ethiopia
Online ISSN 1726-801X

SYNTHESIS, CHARACTERIZATION, AND COMPUTATIONAL ANALYSIS OF CHROMIUM TRIOXIDE AND AMINO ACID-DERIVED METAL COMPLEXES

Nada A. Adam[1], Moamen S. Refat[2*], Amnah Mohammed Alsuhaibani[3], Kareem A. Asla[4] and Abdel Majid A. Adam[2]

[1]Department of Computer Science, The Applied College, Northern Border University, Arar 73213, Saudi Arabia
[2]Department of Chemistry, College of Science, Taif University, P.O. Box 11099, Taif 21944, Saudi Arabia
[3]Department of Sports Health, College of Sport Sciences & Physical Activity, Princess Nourah bint Abdulrahman University, PO Box 84428, Riyadh 11671, Saudi Arabia
[4]Department of Chemistry, Faculty of Science, Zagazig University, Zagazig 44519, Egypt

(Received March 10, 2025; Revised March 20, 2025; Accepted March 21, 2025)

ABSTRACT. This study focused on the preparation and characterization of six metal-based complexes, synthesized through the reaction of chromium trioxide (CrO_3) with a range of different amino acids in a methanol solvent. The amino acids investigated included glycine (Gly), L-alanine (Ala), L-serine (Ser), L-proline (Pro), L-cysteine (Cys), and S-methyl-L-cysteine (MeCys). The synthesis procedure of the CrO_3-Amino acid complexes involved several steps: preparation of individual methanolic solutions of amino acids, addition of CrO_3 solution, refluxing at approximately 65 °C for 3 hours, precipitation, separation, and purification of the final CrO_3-Amino acid complexes. Infrared (FTIR) analysis suggested that the amino acids captured CrO_3 through both amino and carboxylate groups. Thermal analysis offered insights into the two-stage degradation process of the synthesized CrO_3-Amino acid complexes. Finally, the synthesized CrO_3-Amino acid complexes were computationally analyzed, encompassing geometry optimization and energy parameter calculations using the density functional theory (DFT) method. The total energy calculations reveal that the synthesized CrO_3-Amino acid complexes are more stable and have lower total energy compared to their corresponding free amino acids, suggesting the formation of more stable complexes.

KEY WORDS: Metal complexes, Amino acids, CrO_3, Thermal decomposition, Computational calculations, Geometry optimization

INTRODUCTION

Nanotechnology has garnered growing interest and momentum across diverse research disciplines, emerging as a potent and transformative tool within microbiology, medicine, pharmacology, biotechnology, and environmental sciences. Among the extensive range of available nanomaterials, metal and metal oxide nanoparticles are widely utilized in numerous industrial and consumer applications, with some drawing significant attention and investigation due to their remarkable bactericidal capabilities. These versatile nanoparticles have also witnessed increased interest and exploration for a variety of promising applications such as plant protection, wound healing, drug delivery, and bioimaging [1, 2]. Metallic elements can form chemical compounds called metal complexes when they react with specific molecules known as ligands. These complexes are vital in life-saving research. The central metal element binds to the ligands through covalent bonds. The ligands, acting as Lewis bases, donate electrons, while the central metal elements, as Lewis acids, accept these electrons. The ligands can be organic or inorganic, electron-rich molecules that are neutral, positively charged, or negatively charged, with one or more electron pairs to share with metals. Ligands are categorized based on the number of donating atoms as monodentate, bidentate, tridentate, or polydentate [3-7]. Metal complexes possess unique

*Corresponding authors. E-mail: msrefat@tu.edu.sa; msrefat@yahoo.com

spectroscopic, photophysical, electrochemical, and biological properties, including antioxidant, chemotherapeutic, and antimicrobial activities. These properties have the potential to save lives in various fields, such as materials science, medicine, and catalysis [8, 9]. Transition metals are crucial in designing metal-based drugs to treat conditions like cancer, neurological disorders, infections, and diabetes [10, 11]. These complexes are also used in disease diagnosis. Researchers are showing growing interest in metal-based complexes, which play a vital role in studying the interactions between bioactive molecules and metal ions, contributing to the development of innovative metallodrugs [12-21].

Chromium exists in three primary forms: metallic ore, trivalent chromium (Cr^{3+}), and hexavalent chromium (Cr^{6+}). Trivalent chromium is found naturally in various fresh foods, including yeasts, grains, meats, fruits, and vegetables. It is the predominant form present in surface soils, where oxidation processes convert chromium from the hexavalent to the trivalent state. Hexavalent chromium also occurs naturally, particularly in water-saturated environments, and can serve as an indicator of human-induced pollution. This form is relatively soluble and can readily migrate through soil to groundwater, potentially presenting environmental and health risks [22]. Chromium(VI) oxide, also known as chromium trioxide, is a chemical compound with the formula CrO_3. It is a highly versatile oxidizing agent and is suspected to be carcinogenic. This compound has a wide range of industrial and commercial applications, leveraging its diverse properties and functionalities. When dissolved in water, it generates chromic acid and can react with various oxidizable organic compounds. Chromium(VI) oxide is typically produced by treating sodium chromate with sulfuric acid. Large quantities are manufactured annually for use in electroplating processes, where it is employed to deposit a protective and decorative chrome coating on metal surfaces. Additionally, chromium(VI) oxide has diverse applications, including in aerospace engineering, the production of synthetic rubies, and chrome plating, which enhances the appearance and corrosion resistance of metallic objects [23].

This study focused on the preparation and characterization of six metal-based complexes, which were synthesized through the reaction of chromium trioxide (CrO_3) with a range of different amino acids in a methanol solvent. The amino acids investigated included glycine (Gly), L-alanine (Ala), L-serine (Ser), L-proline (Pro), L-cysteine (Cys), and S-methyl-L-cysteine (MeCys). The resulting CrO_3-amino acid complexes were computationally analyzed, encompassing geometry optimization and energy parameter calculations using the DFT method.

EXPERMENTAL

Chemicals

All the chemicals were purchased from Fluka (Seelze, Germany), Merck KGaA (Darmstadt, Germany), and Sigma-Aldrich (St Louis, MO, USA) Chemical Companies and were utilized without further modification or purification. They were of the highest reagent grade available and were used as received, without any additional processing or preparation. Chromium trioxide (CrO_3; 99.99 g/mol; purity ≥ 98.0%) was obtained from Sigma-Aldrich. The amino acids investigated in this study were glycine, L-alanine, L-serine, L-proline, L-cysteine, and S-methyl-L-cysteine, which were provided by Merck KGaA. The IUPAC names, abbreviations, chemical formulas, and structures of the amino acids were listed in Table 1. HPLC-grade methanol was purchased from Fluka.

Synthesis of CrO_3-Amino acid complexes

The CrO_3-Amino acid complexes were synthesized using the following procedure: First, six 100-mL beakers labeled A, B, C, D, E, and F were prepared, each containing 3 mmol of the amino acids Gly, Ala, Ser, Pro, Cys, and MeCys, respectively. The amino acids were dissolved in 25 mL

of methanol, and gentle heating was employed to ensure complete dissolution. Second, a hot 25 mL methanolic solution containing 3 mmol of CrO_3 was gradually added to each beaker. The six systems, CrO_3-Gly, CrO_3-Ala, CrO_3-Ser, CrO_3-Pro, CrO_3-Cys, and CrO_3-MeCys, were then transferred to reflux systems. Third, the mixtures were refluxed on a hotplate at approximately 65 °C for 3 hours under stirring. After cooling, reddish-brown precipitates were generated. To ensure complete precipitation of the complexes, all the systems were left overnight. The CrO_3-Gly, CrO_3-Ala, CrO_3-Ser, CrO_3-Pro, CrO_3-Cys, and CrO_3-MeCys products were then separated from the systems. Finally, the products were purified by thoroughly washing with methanol and diethyl ether, and the pure CrO_3-Amino acid complexes were dried in vacuum desiccators over anhydrous $CaCl_2$ for 48 hours.

Compositions

The compositions of the CrO_3-Gly, CrO_3-Ala, CrO_3-Ser, CrO_3-Pro, CrO_3-Cys, and CrO_3-MeCys products were determined through comprehensive elemental analyses data collected using a Perkin-Elmer 2400 series II CHNS Elemental Analyzer. The percentages of carbon, hydrogen, and nitrogen obtained from this instrument were then carefully used to propose the chemical formulas for the synthesized CrO_3-amino acid complexes.

Table 1. The abbreviations, molecular weights, chemical formulas, and chemical structures of the investigated amino acids.

Amino acid	Abbreviation	IUPAC name	Chemical structure	Chemical formula
Glycine	Gly	Aminoacetic acid	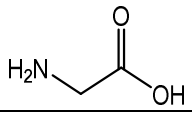	$C_2H_5NO_2$ (75.07 g/mol)
L-Alanine	Ala	(*S*)-2-Aminopropionic acid	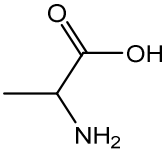	$C_3H_7NO_2$ (89.09 g/mol)
L-Serine	Ser	(S)-2-Amino-3-hydroxypropionic acid	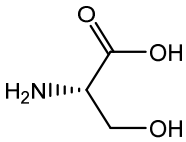	$C_3H_7NO_3$ (105.09 g/mol)
L-Proline	Pro	(*S*)-Pyrrolidine-2-carboxylic acid	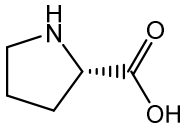	$C_5H_9NO_2$ (115.13 g/mol)

L-Cysteine	Cys	(*R*)-2-Amino-3-mercaptopropionic acid	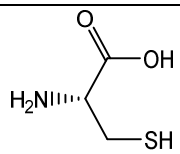	$C_3H_7NO_2S$ (121.15 g/mol)
S-Methyl-L-cysteine	MeCys	2-Amino-3-(methylthio)propanoic acid	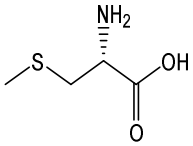	$C_4H_9NO_2S$ (135.18 g/mol)

Mode of interactions and complex structure

The modes of interactions and the chelating properties of the amino acids toward the CrO_3, as well as the complex structure, were determined based on Fourier-transform infrared spectra recorded on the solid state using a Nicolet iS10 FT-IR spectrometer (Thermo Scientific) in the wavenumber range of (4000-400 cm^{-1}) measured at room temperature.

Thermal properties

The thermal decomposition properties of the synthesized CrO_3-amino acid complexes were investigated using a Shimadzu TGA–50H thermal analyzer under an air atmosphere. The study included thermogravimetric (TG) measurements within the specified temperature range (25-800 ºC). Alumina powder was used as the reference material, and standard platinum pans were employed for the measurements.

Computational calculations

The computational investigations, which encompassed geometry optimization, were conducted using the DMOL^3 program from the Materials Studio package. The DFT semi-core pseudopotential computations (dspp) were performed with Double numerical basis sets and the polarization functional (DNP). The generalized gradient approximation (GGA), which is the preferred correlation functional, serves as the foundation for the RPBE functional. These computational analyses were crucial for comprehending the structural and electronic characteristics of the complexes under study [24-26].

RESULTS AND DISCUSSION

Compositions

This study focused on the preparation and characterization of six metal-based complexes containing CrO_3 and amino acids. The amino acids investigated were glycine (Gly), L-alanine (Ala), L-serine (Ser), L-proline (Pro), L-cysteine (Cys), and S-methyl-L-cysteine (MeCys). The synthesis of the CrO_3-amino acid complexes involved several steps, including the preparation of individual amino acid solutions, the addition of CrO_3 methanolic solution, refluxing, precipitation, separation, and purification of the final CrO_3-amino acid complexes. The compositions of the purified and dried CrO_3-Gly, CrO_3-Ala, CrO_3-Ser, CrO_3-Pro, CrO_3-Cys, and CrO_3-MeCys complexes were determined through comprehensive elemental analyses using a Perkin-Elmer 2400 series II CHNS Elemental Analyzer. The percentages of carbon, hydrogen, nitrogen, and

sulfur obtained were then carefully used to propose the chemical formulas for the synthesized CrO_3-amino acid complexes. The chromium element content in the complexes was determined using a gravimetric technique. The compositions for each CrO_3-amino acid complex, including the quantities of C, N, S, H, and Cr, are described in detail below.

i) CrO_3-Gly complex: this compound has the chemical formula of $C_2H_5NO_2CrO_3$ and a molecular weight of 175.06 g/mol. Elemental analysis reveals the following observed percentages: C, 13.95; N, 7.82; H, 3.00; and Cr, 29.52. The theoretically calculated percentages were C, 13.71; N, 8.00; H, 2.86; and Cr, 29.70. ii) CrO_3-Ala complex: this compound has the chemical formula of $C_3H_7NO_2CrO_3$ and a molecular weight of 189.08 g/mol. Elemental analysis reveals the following observed percentages: C, 19.15; N, 7.66; H, 3.84; and Cr, 27.31. The theoretically calculated percentages were C, 19.04; N, 7.40; H, 3.70; and Cr, 27.50. iii) CrO_3-Ser complex: this compound has the chemical formula of $C_3H_7NO_3CrO_3$ and a molecular weight of 205.08 g/mol. Elemental analysis reveals the following observed percentages: C, 17.77; N, 6.95; H, 3.29; and Cr, 25.60. The theoretically calculated percentages were C, 17.55; N, 6.82; H, 3.41; and Cr, 25.36. iv) CrO_3-Pro complex: this compound has the chemical formula of $C_5H_9NO_2CrO_3$ and a molecular weight of 215.12 g/mol. Elemental analysis reveals the following observed percentages: C, 28.00; N, 6.29; H, 4.45; and Cr, 24.00. The theoretically calculated percentages were C, 27.89; N, 6.51; H, 4.18; and Cr, 24.17. v) CrO_3-Cys complex: this compound has the chemical formula of $C_3H_7NO_2SCrO_3$ and a molecular weight of 221.14 g/mol. Elemental analysis reveals the following observed percentages: C, 16.53; N, 6.15; H, 2.96; S, 14.35; and Cr, 23.73. The theoretically calculated percentages were C, 16.28; N, 6.33; H, 3.17; S, 14.47; and Cr, 23.51. vi) CrO_3-MeCys complex: this compound has the chemical formula of $C_4H_9NO_2SCrO_3$ and a molecular weight of 235.17 g/mol. Elemental analysis reveals the following observed percentages: C, 20.18; N, 6.19; H, 3.70; S, 13.85; and Cr, 22.37. The theoretically calculated percentages were C, 20.41; N, 5.95; H, 3.83; S, 13.61; and Cr, 22.11.

Analysis of the elemental data for carbon (C), hydrogen (H), nitrogen (N), and sulfur (S), as well as the chromium metal content revealed that the reaction of CrO_3 with all amino acids proceeded via a 1:1 molar ratio (CrO_3 to amino acid). Based on this molar ratio, the general composition of the synthesized complexes is [CrO_3(Amino acid)]. The gross formulas of CrO_3-Gly, CrO_3-Ala, CrO_3-Ser, CrO_3-Pro, CrO_3-Cys, and CrO_3-MeCys complexes are $C_2H_5NO_2CrO_3$ (175.06 g/mol), $C_3H_7NO_2CrO_3$ (189.08 g/mol), $C_3H_7NO_3CrO_3$ (205.08 g/mol), $C_5H_9NO_2CrO_3$ (215.12 g/mol), $C_3H_7NO_2SCrO_3$ (221.14 g/mol), and $C_4H_9NO_2SCrO_3$ (235.17 g/mol), respectively.

Mode of interactions and complex structure

At room temperature, solid amino acids take on a zwitterionic form, with a protonated amino group and a deprotonated carboxyl group. The amino acid molecule can either gain or lose a hydrogen ion, resulting in a positively or negatively charged state, respectively. The zwitterionic structure is characteristic of amino acids in solution and is a crucial feature that enhances their water solubility and facilitates their participation in a wide range of biochemical reactions and interactions within living organisms. This zwitterionic structure, with a positively charged amino group (NH_3^+) and a negatively charged carboxyl (COO^-) group, is a key feature of amino acids that allows them to maintain a neutral, balanced state at physiological pH. This distinctive property facilitates the ready dissolution of amino acids in water and their participation in a broad range of biological processes, such as protein synthesis, enzyme catalysis, and cellular signaling. Free amino acids exhibit distinct infrared (FTIR) bands corresponding to the stretching vibrations of the ammonium and carboxylate groups, typically found in the broad regions of 2600 and 1600 cm^{-1}, respectively.

The FT-IR spectral features of the free amino acid molecules examined in this study are described in detail below. These IR data are consistent with and corroborate the findings of

previous investigations in this field [27-29]. The characteristic FT-IR bands (cm^{-1}) of the free Gly molecule were observed at 3440 $\nu(NH_3^+)$, 2794 $\nu_{as}(CH_2)$, 2598 $\nu_s(CH_2)$, 1624, 1512 $\delta(NH_3^+)$ and $\nu(COO^-)$, 1489 $\nu(COO^-)$, 1436 $\delta(CH_2)$, 1410 $\nu(COO^-)$, 1396, 1323 $\omega(CH_2)$ and $\omega(NH_3^+)$, 1126 $\rho(NH_3^+)$, 1153, 1039 $\nu(CN)$, 929 $\rho(CH_2)$, 889 $\nu(CCC)$, 686 $\omega(COO^-)$, 607 $\delta(COO^-)$, 584 and 501 $\delta(CCO^-)$ and $\nu(CN)$. The characteristic FT-IR spectral features (cm^{-1}) of the free Ala molecule were observed at 3099 $\nu(NH_3^+)$, 2926 $\nu(CH_3)$, 1595, 1460 $\delta(NH_3^+)$ and $\nu(COO^-)$, 1455 $\delta_{as}(CH_3)$, 1412, $\delta_s(CH_3)$, and $\delta(NCH)$, 1376 $\delta_s(CH_3)$, 1363 $\nu(COO^-)$, $\delta(NCH)$, and $\delta(CCC)$, 1307 $\delta(CCH)$, 1237 $\rho(NH_3^+)$, 1206 $\delta_s(COH)$, 1152 $\rho(NH_3^+)$ and $\delta(CCH)$, 1114 $\nu(CN)$, 1014 $\nu(C\text{-}CH_3)$, $\rho(NH_3^+)$, and $\rho(CH_3)$, 919 $\nu(CNH)$ and $\nu(CCC)$, 850 $\nu(CN)$ and $\nu(CCC)$, $\nu(C\text{-}OO)$, 772 $\omega(COO^-)$, 649 $\delta(COO^-)$, $\rho(NH_3^+)$, and $\rho(CH_3)$, 540 $\delta(CCO^-)$ and $\nu(CN)$. For the free Ser molecule, the characteristic FT-IR bands (cm^{-1}) were observed at 3456 $\nu(OH)$, 3010 $\nu(NH_3^+)$, 2997 $\nu_{as}(CH_2)$, 2956, 2906 $\nu_s(CH_2)$ and $\nu(CH)$, 1638, 1623, 1605 $\delta(NH_3^+)$, 1590 $\nu(COO^-)$, 1495, 1480 $\delta(NH_3^+)$, 1470, 1425 $\delta(CH_2)$, 1411 $\nu(COO^-)$, 1383 $\omega(CH_2)$, 1341 $\delta(CH)$, 1310 $\rho(CH)$, 1218 $\delta(COH)$, 1127 $\rho(NH_3^+)$, 1086 $\nu(CN)$, 1013 $\nu(CN)$, 968 $\rho(CH_2)$, 919, 853 $\nu(CCC)$, 803 $\omega(COO^-)$, $\omega(COO^-)$, 612 $\delta(COO^-)$. For the free Pro molecule, the characteristic FT-IR bands (cm^{-1}) were observed at 3417 $\nu(NH_2^+)$, 3062 $\nu_{as}(CH_2)$, 2985 $\nu_s(CH_2)$ and $\nu(CH)$, 1624 $\delta(NH_2^+)$, 1565 $\nu(COO^-)$, 1447 $\delta(CH_2)$, 1408 $\nu(COO^-)$, 1330 $\delta(CH)$, 1288 $\omega(CH_2)$, 1169, 1088 $\rho(CH_2)$ and $\delta(CH)$, 1043 $\nu(CC)$, 995 $\nu(CCN)$ and $\nu(CC)$, 947 $\rho(CH_2)$, 847 $\rho(NH_2^+)$, 783 $\rho(NH_2^+)$ and $\nu(CCC)$, $\nu(CCC)$, 679 $\delta(COO^-)$ and $\nu(CN)$, 630 $\delta(COO^-)$, 459 $\rho(COO^-)$. Characteristic FT-IR spectral signatures (cm^{-1}) of the free Cys molecule were detected at 3165, 3068 $\nu(NH_3^+)$, 2960 $\nu_{as}(CH_2)$, 2920 $\nu_s(CH_2)$ and $\nu(CH)$, 2638 $\nu(NH_3^+)$, 2552, 2362 $\nu(SH)$, 1610 $\nu(COO^-)$, 1586, 1541 $\delta(NH_3^+)$, 1485 $\delta(CH_2)$, 1394 $\omega(CH_2)$, 1338 $\delta(CH)$, 1296 $\rho(CH)$, 1268 $\delta(COH)$, 1137 $\rho(NH_3^+)$, 1125 $\nu(CCC)$, 1091 $\nu(CN)$, 1064 $\rho(NH_3^+)$, 1035 $\nu(CN)$, 1003 $\delta(SH)$, 943 $\nu(N\text{-}CH)$, 867 $\nu(CC)$, 823 $\omega(COO^-)$, 806 $\delta(COO^-)$, 695 $\nu(C\text{-}S)$, 538 $\delta(CCO^-)$. For the free MeCys molecule, the FT-IR spectral signatures (cm^{-1}) were detected at 3004 $\nu(NH_3^+)$, 2994 $\nu_{as}(CH_3)$ and $\nu_{as}(CH_2)$, 2922 $\nu_s(CH_2)$ and $\nu(CH)$, 2608 $\nu(NH_3^+)$, 1620 $\nu(COO^-)$, 1582 $\delta(NH_3^+)$, 1486 $\delta_{as}(CH_3)$, 1416 $\delta(CH_2)$, 1391 $\omega(CH_2)$, 1344 $\delta(CH)$, 1320 $\delta_s(CH_3)$, 1300 $\rho(CH)$, 1267 $\delta(CCH)$, 1206 $\delta(COH)$, 1130 $\rho(NH_3^+)$, 1103 $\nu(CN)$, 1066 $\rho(NH_3^+)$, 1035 $\nu(CN)$, 961 $\nu(N\text{-}CH)$, 950 $\rho(CH_3)$, 881 $\nu(CC)$, 847 $\omega(COO^-)$, 783 $\delta(COO^-)$, 730 $\omega(COO^-)$, 678 $\nu(C\text{-}S)$, 613 $\rho(CH_3)$, 543 $\delta(CCO^-)$, 466 $\rho(COO^-)$.

Figure 1 shows the FT-IR spectra of the CrO_3-Gly, CrO_3-Ala, CrO_3-Ser, CrO_3-Pro, CrO_3-Cys, and CrO_3-MeCys complexes. The free amino acids Gly, Ala, Ser, Pro, Cys, and MeCys exhibit characteristic IR bands originating from the stretching vibrations of the ammonium and carboxylate groups, typically found in the regions of 3440-3000 cm^{-1} and 1620-1512 cm^{-1}, respectively, in their FT-IR spectra. These characteristic absorption bands were significantly altered upon coordination with CrO_3, forming the CrO_3-Gly, CrO_3-Ala, CrO_3-Ser, CrO_3-Pro, CrO_3-Cys, and CrO_3-MeCys complexes. The free Gly molecule exhibited a vibrational stretching band at 3440 cm^{-1} due to the ammonium group, which shifted to 3350 cm^{-1} when it formed a complex with CrO_3. Furthermore, the two carboxylate stretching bands of free Gly at 1512 cm^{-1} and 1489 cm^{-1} changed to 1500 cm^{-1} and 1454 cm^{-1} upon complexation with CrO_3. The free Ala molecule displayed a vibrational stretching band at 3099 cm^{-1}, which was attributed to the ammonium group. This band shifted to 3255 cm^{-1} when the Ala molecule formed a complex with CrO_3. Additionally, the two carboxylate stretching bands of the free Ala molecule, observed at 1595 cm^{-1} and 1460 cm^{-1}, changed to 1573 cm^{-1} and 1448 cm^{-1} upon complexation with CrO_3. The unbound Ser molecule exhibited a vibrational stretching band at 3010 cm^{-1}, which was attributed to the ammonium group. This band shifted to 3300 cm^{-1} when the Ser molecule formed a complex with CrO_3. Furthermore, the two carboxylate stretching bands of the unbound Ser molecule, observed at 1590 cm^{-1} and 1495 cm^{-1}, changed to 1618 cm^{-1} and 1480 cm^{-1} upon complexation with CrO_3. The characteristics of the bands originating from the ammonium group were shifted from 3417, 3165, and 3004 cm^{-1} in free Pro, Cys, and MeCys, respectively, to 3337,

3210, and 3320 cm^{-1} in the Pro-CrO_3, Cys-CrO_3, and MeCys-CrO_3 complexes, respectively. The two carboxylate stretching bands of free Pro, Cys, and MeCys were located at (1565 and 1408 cm^{-1}), (1610 and 1541) and (1620 and 1540 cm^{-1}), respectively. However, in the Pro-CrO_3, Cys-CrO_3, and MeCys-CrO_3 complexes, these bands appeared at (1540 and 1426 cm^{-1}), (1588 and 1560 cm^{-1}) and (1595 and 1518 cm^{-1}), respectively. The formation of CrO_3-amino acid complexes indicates that the free amino acids can act as ligands, coordinating to the CrO_3 through their amino and carboxylate functional groups. This coordination leads to the observed changes in the characteristic IR bands, as the vibrations of these groups are influenced by the presence of the CrO_3 moiety. The bands appeared at 586, 560, 588, 594, 586, and 557 cm^{-1} in the FT-IR spectra of the CrO_3-Gly, CrO_3-Ala, CrO_3-Ser, CrO_3-Pro, CrO_3-Cys, and CrO_3-MeCys complexes, respectively, could be assigned to ν(Cr–O) vibrational modes. These complexes also showed absorption bands at 528, 525, 533, 542, 540, and 530 cm^{-1} arising from the ν(Cr–N) vibrational modes [30, 31]. The collected elemental and FT-IR spectral data were utilized to propose the chemical structures of the synthesized CrO_3-amino acid complexes, as shown in Figure 2.

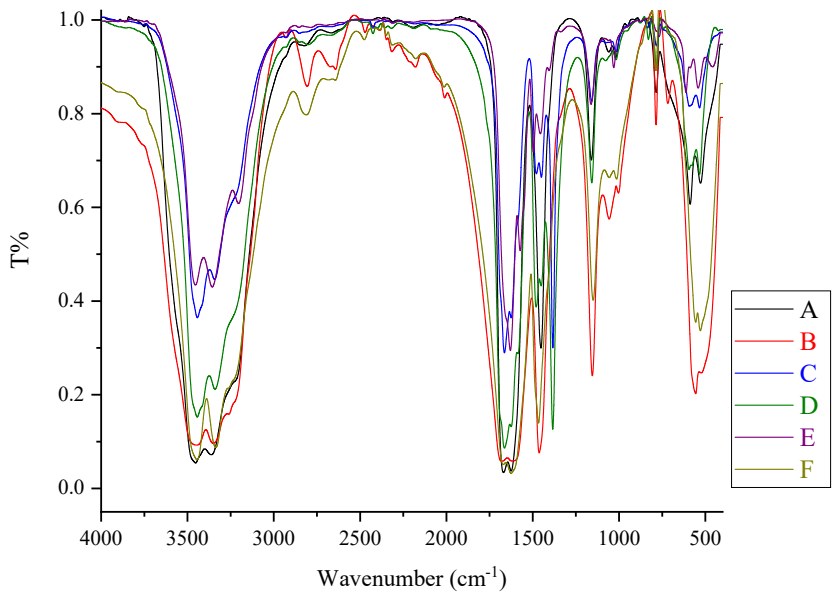

Figure 1. FT-IR spectra of **A**) CrO_3-Gly complex, **B**) CrO_3-Ala complex, **C**) CrO_3-Ser complex, **D**) CrO_3-Pro complex, **E**) CrO_3-Cys complex, and **F**) CrO_3-MeCys complex.

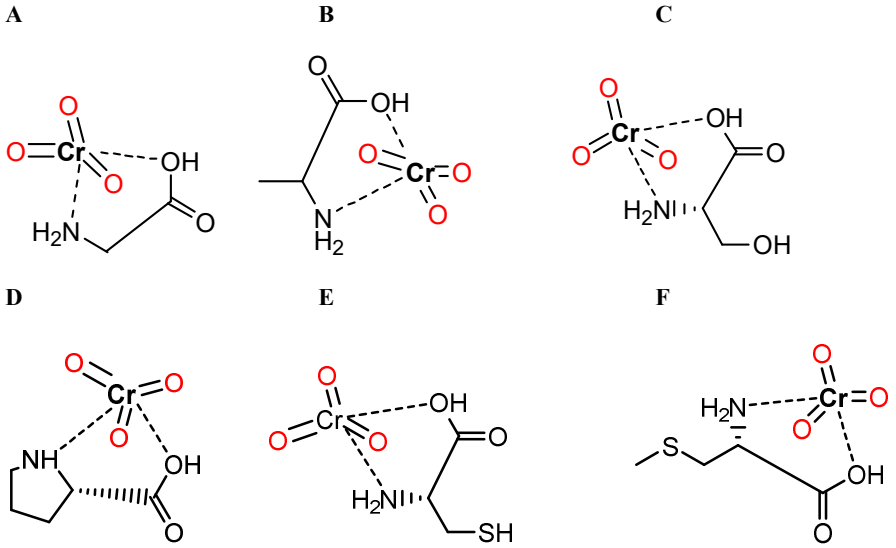

Figure 2. Proposed chemical structures of the synthesized CrO_3-amino acid complexes: **A**) CrO_3-Gly complex, **B**) CrO_3-Ala complex, **C**) CrO_3-Ser complex, **D**) CrO_3-Pro complex, **E**) CrO_3-Cys complex, and **F**) CrO_3-MeCys complex.

Thermal properties

The thermal decomposition properties of the synthesized CrO_3-amino acid complexes were thoroughly investigated using a Shimadzu TGA–50H thermal analyzer under an air atmosphere. Thermogravimetric (TG) measurements were meticulously conducted within the specified temperature range from 25 °C to 800 °C. The detailed thermograms presented in Figure 3 show that all the CrO_3-amino acid complexes undergo a two-step decomposition process. The CrO_3-Gly complex decomposed in the distinct temperature ranges of 50–260 °C and 260–550 °C. The CrO_3-Ala complex decomposed in the separate temperature ranges of 50–255 °C and 255–500 °C. The CrO_3-Ser complex decomposed in the specific temperature ranges of 55–225 °C and 225–500 °C. The CrO_3-Pro complex decomposed in the distinct temperature ranges of 60–275 °C and 275–550 °C. The CrO_3-Cys complex decomposed in the separate temperature ranges of 75–250 °C and 250–675 °C. The CrO_3-MeCys complex decomposed in the specific temperature ranges of 150–300 °C and 300–650 °C. The comprehensive degradation of the synthesized CrO_3-amino acid complexes was ultimately completed by leaving $\frac{1}{2}Cr_2O_3$ free of any residual carbons as the final decomposition product. The CrO_3-Gly complex fully decomposed at approximately 550 °C, resulting in a 43.25% weight loss of $\frac{1}{2}Cr_2O_3$ as the final thermal product. The CrO_3-Ala complex underwent complete decomposition at around 500 °C, resulting in a 40.0% weight loss of $\frac{1}{2}Cr_2O_3$ as the final thermal product. The CrO_3-Ser complex decomposed completely at roughly 500 °C, resulting in a 37.18% weight loss of $\frac{1}{2}Cr_2O_3$ as the final thermal product. The CrO_3-Pro complex decomposed fully at about 550 °C, resulting in a 35.62% weight loss of $\frac{1}{2}Cr_2O_3$ as the final thermal product. The CrO_3-Cys complex underwent complete decomposition at approximately 675 °C, resulting in a 34.50% weight loss of $\frac{1}{2}Cr_2O_3$ as the final thermal product. The CrO_3-MeCys complex decomposed completely at around 650 °C, resulting in a 32.71% weight loss of $\frac{1}{2}Cr_2O_3$ as the final thermal product.

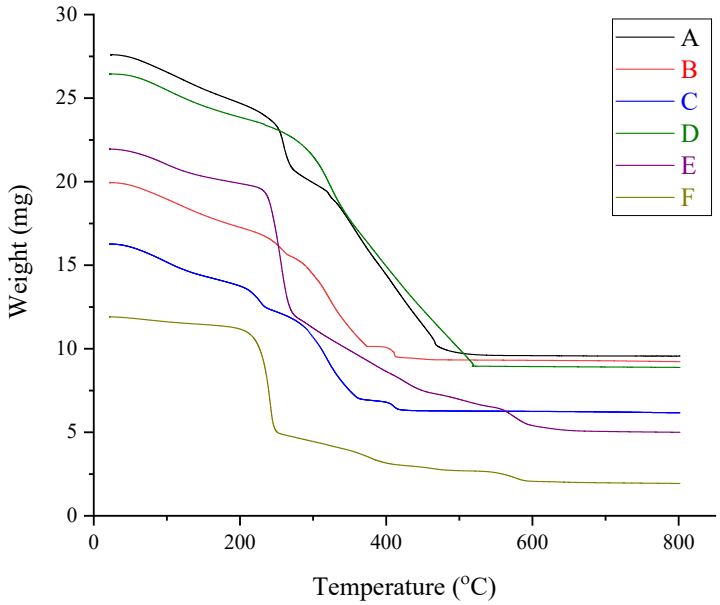

Figure 3. Thermograms of **A**) CrO_3-Gly complex, **B**) CrO_3-Ala complex, **C**) CrO_3-Ser complex, **D**) CrO_3-Pro complex, **E**) CrO_3-Cys complex, and **F**) CrO_3-MeCys complex.

Computational calculations

Using the density functional theory (DFT) method, the molecular geometries of the free amino acids and the synthesized CrO_3-amino acid complexes were optimized using a (dnp) basis set. Additionally, various energetic parameters were estimated, including total energy, frontier molecular orbitals (E_{HOMO} and E_{LUMO}), molecular dipolar moments (μ), energy band gap, and binding energy. Tables 2 and 3 list the calculated E_{HOMO}, E_{LUMO}, energy band gap (E_H–E_L), total energy, binding energy, and dipole moment for the free amino acids and the synthesized complexes, respectively. The optimized molecular structures of the CrO_3-Amino acid complexes were displayed in the ground state and illustrated in Figure 4. Figures 5 and 6 depict the optimized geometries of the HOMO and LUMO, respectively, for the synthesized CrO_3-Amino acid complexes. The optimized geometry predicts a square pyramidal geometry with dsp^3 hybridization for all the complexes. The data presented in Tables 2 and 3 indicate that the calculated energy parameters are negative, suggesting the synthesized CrO_3-Amino acid complexes are stable. The HOMO, which is the electron donor, and the LUMO, which is the electron acceptor, are important parameters for understanding chemical reactivity and stability. The gap between the HOMO and LUMO levels characterizes molecular chemical stability. As this energy gap increases, the compound becomes more chemically stable, as it becomes more difficult for electrons to be excited from the HOMO to the LUMO. The smaller values of the ΔE band gap (eV) for all CrO_3-Amino acid complexes compared to the corresponding free amino acids indicate the stability and enhanced structural integrity of the synthesized complexes. Among the synthesized complexes, the CrO_3-MeCys complex exhibits the smallest ΔE band gap value.

This smaller energy gap facilitates more efficient charge transfer, which can ultimately impact the bioactivity and potential therapeutic applications of the complex. The higher HOMO energy values observed for all the synthesized complexes, compared to the corresponding HOMO energy values of the free amino acids, indicate that it is easier to remove an electron from the CrO_3-Amino acid complex than the free amino acid, suggesting increased reactivity. This increased reactivity may be attributed to the formation of a stable complex between the CrO_3 and the amino acid, which can facilitate the removal of an electron from the system more readily than the free amino acid alone [32]. The calculations of the binding energy (eV) for the free amino acids and their corresponding complexes with CrO_3 demonstrate that all complexes have higher binding energy values compared to the free amino acids. This indicates that the synthesized complexes possess greater stability and are more energetically favorable than the free amino acids [32]. Furthermore, the total energy calculations reveal that the synthesized CrO_3-Amino acid complexes are more stable and have lower total energy compared to their corresponding free amino acids, suggesting the formation of more stable complexes.

Table 2. Calculated E_{HOMO}, E_{LUMO}, energy band gap (E_H–E_L), total energy, binding energy, and dipole moment for the free amino acids, as determined using the DMOL^3 method and the DFT approach.

Amino acid	E_{HOMO} (eV)	E_{LUMO} (eV)	$\Delta E_{band\ gap}$	Total energy (eV)	Binding energy (eV)	Dipole moment (Debye)
Gly	5.52	0.853	4.667	-7743.090016	-42.91819	3.1265
Ala	5.517	0.983	4.534	-8813.203404	-55.70042	3.2222
Ser	5.542	0.993	4.549	-10860.73068	-60.25656	1.2524
Pro	4.912	0.792	4.12	-10920.39891	-75.62428	3.8518
Cys	5.339	1.324	4.015	-19648.0643	-57.65117	1.0681
MeCys	4.942	1.299	3.643	-20718.26046	-70.34394	1.8122

Table 3. Calculated E_{HOMO}, E_{LUMO}, energy band gap (E_H–E_L), total energy, binding energy, and dipole moment for the synthesized complexes, as determined using the DMOL^3 method and the DFT approach.

Complex	E_{HOMO} (eV)	E_{LUMO} (eV)	$\Delta E_{band\ gap}$	Total energy (eV)	Binding energy (eV)	Dipole moment (Debye)
CrO_3-Gly	6.656	3.808	2.848	-16708.11472	-69.27228	10.3983
CrO_3-Ala	6.665	3.781	2.884	-17778.63571	-82.21195	11.3813
CrO_3-Ser	6.466	3.617	2.849	-19826.51344	-87.06608	15.3851
CrO_3-Pro	6.432	3.579	2.853	-19886.21462	-102.10535	14.5677
CrO_3-Cys	6.504	3.587	2.917	-28614.2432	-85.4734	14.912
CrO_3-MeCys	6.24	3.51	2.73	-29684.72228	-98.37114	18.9415

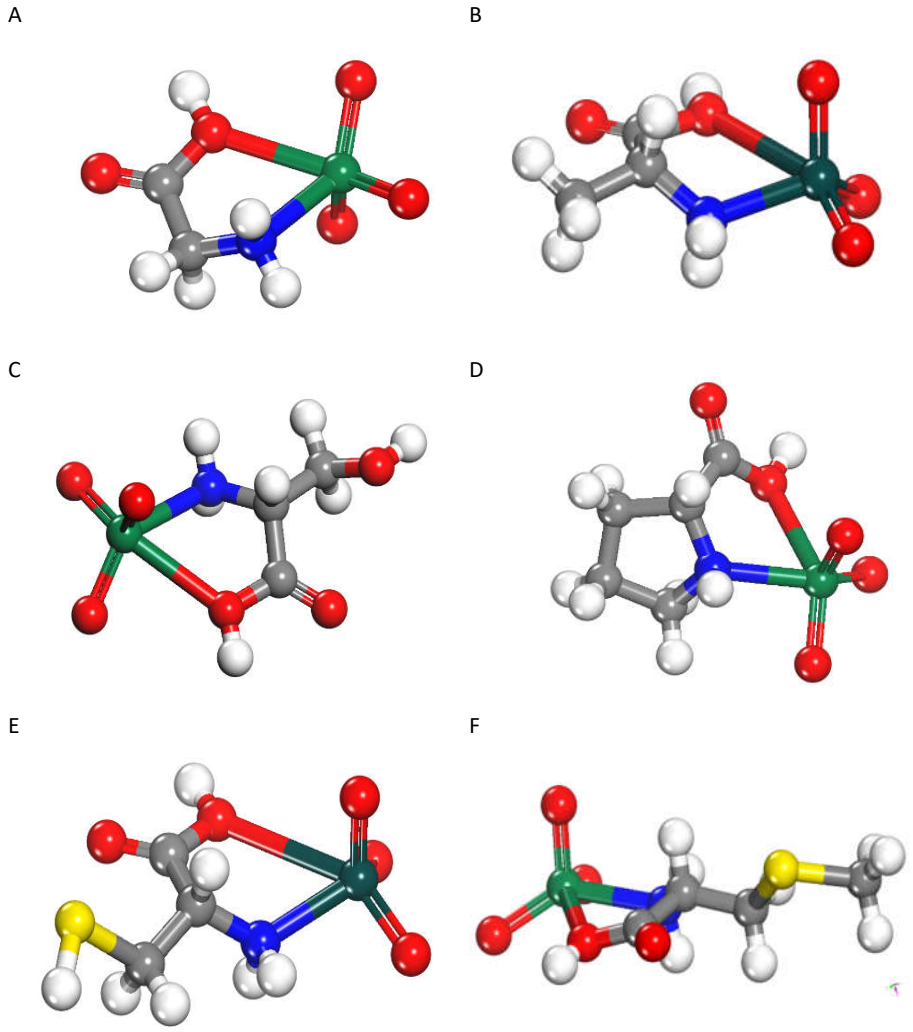

Figure 4. The optimized geometry of the CrO_3-Amino acid complexes: **A**) CrO_3-Gly complex, **B**) CrO_3-Ala complex, **C**) CrO_3-Ser complex, **D**) CrO_3-Pro complex, **E**) CrO_3-Cys complex, and **F**) CrO_3-MeCys complex.

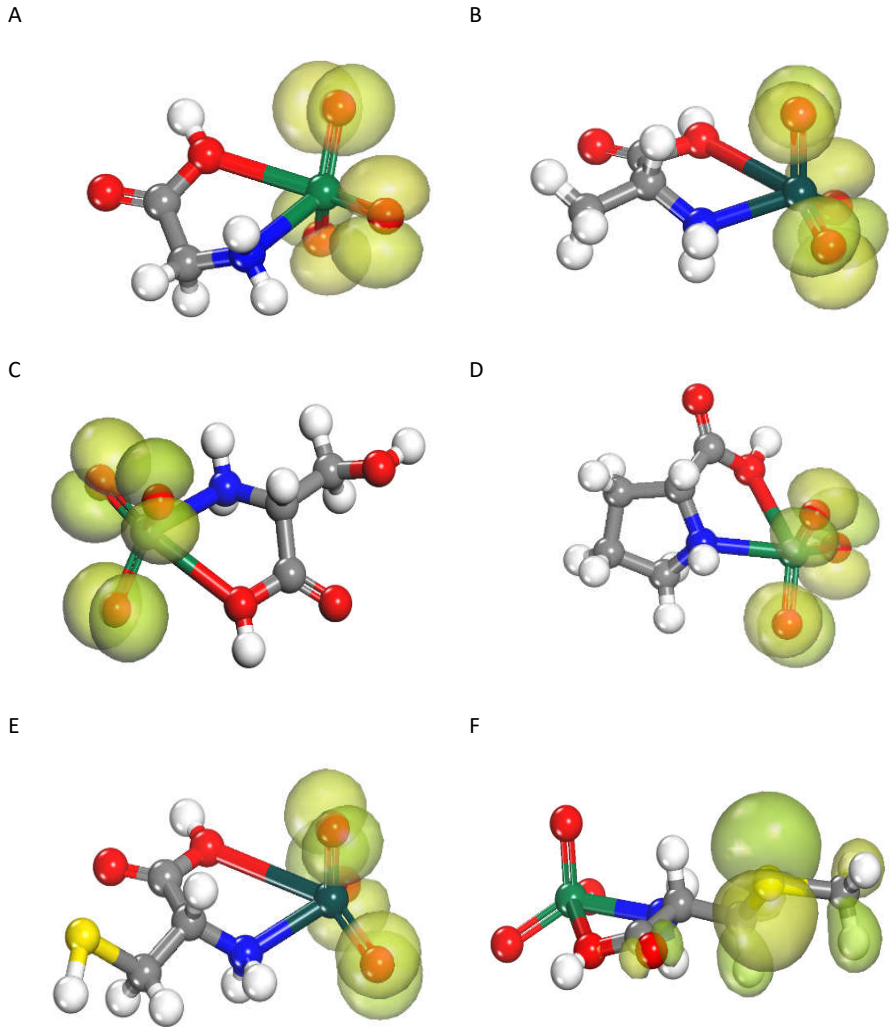

Figure 5. Optimized geometry of the HOMO for the CrO_3-Amino acid complexes: **A**) CrO_3-Gly complex, **B**) CrO_3-Ala complex, **C**) CrO_3-Ser complex, **D**) CrO_3-Pro complex, **E**) CrO_3-Cys complex, and **F**) CrO_3-MeCys complex.

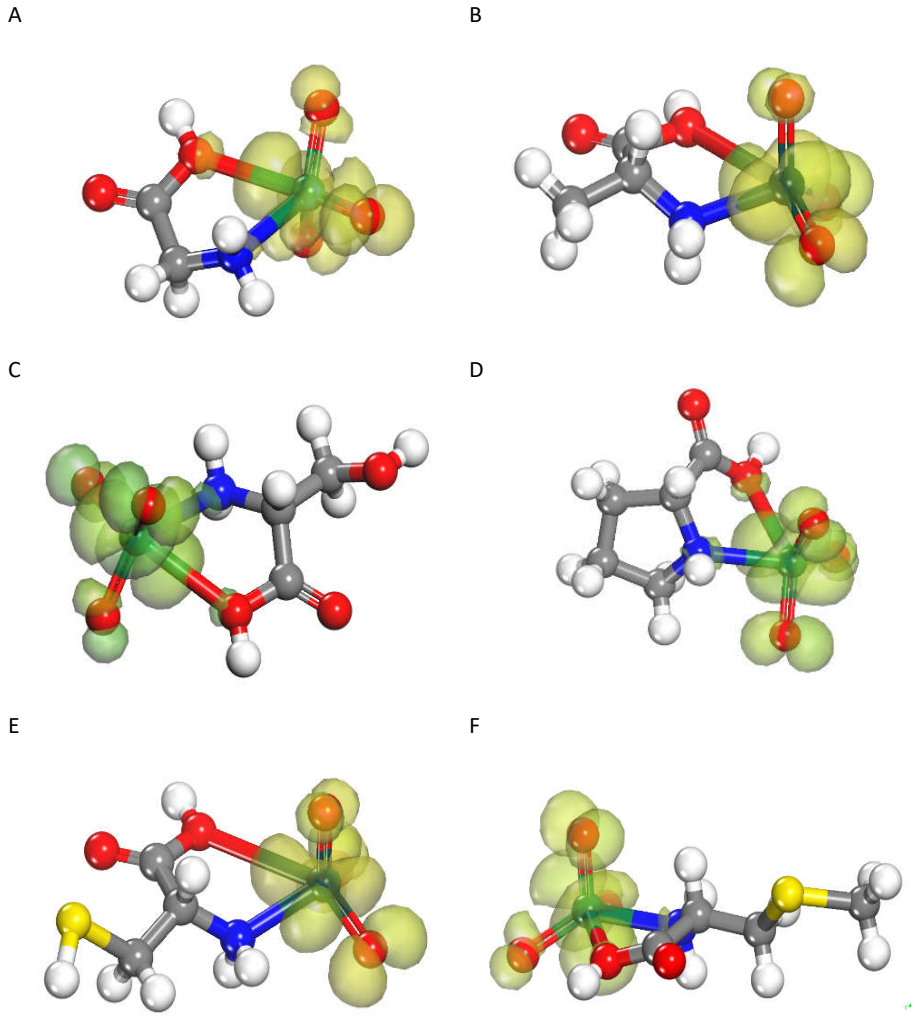

Figure 6. Optimized geometry of the LUMO for the CrO_3-Amino acid complexes: **A**) CrO_3-Gly complex, **B**) CrO_3-Ala complex, **C**) CrO_3-Ser complex, **D**) CrO_3-Pro complex, **E**) CrO_3-Cys complex, and **F**) CrO_3-MeCys complex.

CONCLUSION

This investigation explored the preparation and characterization of six metal-based complexes, which were synthesized through the reaction of chromium trioxide (CrO_3) with a variety of amino acids in a methanol solvent. The analyzed amino acids included glycine (Gly), L-alanine (Ala), L-serine (Ser), L-proline (Pro), L-cysteine (Cys), and S-methyl-L-cysteine (MeCys). The synthesis process of the CrO_3-Amino acid complexes involved several steps: creating individual methanolic solutions of amino acids, adding CrO_3 solution, refluxing at approximately 65 °C for

3 hours, precipitating, separating, and purifying the final CrO_3-Amino acid complexes. Infrared (FTIR) analysis indicated that the amino acids captured CrO_3 through both amino and carboxylate groups. Thermal analysis provided insights into the two-stage degradation process of the synthesized CrO_3-Amino acid complexes. Finally, the synthesized CrO_3-Amino acid complexes were computationally analyzed, including geometry optimization and energy parameter calculations using the density functional theory (DFT) method. The total energy calculations revealed that the synthesized CrO_3-Amino acid complexes are more stable and have lower total energy compared to their corresponding free amino acids, suggesting the formation of more stable complexes. This study provides a comprehensive understanding of the synthesis and analysis of these innovative metal-based amino acid complexes. The versatility of these metal-based complexes enables their potential incorporation into a wide array of applications, including catalytic processes, pharmaceutical development, advanced material design, and other emerging fields.

ACKNOWLEDGEMENT

The authors extend their appreciation to Taif University, Saudi Arabia, for supporting this work through project number (TU-DSPP-2024-6).

Funding

This research was funded by Taif University, Saudi Arabia, Project No. (TU-DSPP-2024-6).

REFERENCES

1. Svensson, F.G.; Simon, P.; Kessler, V.G. Modeling metal oxide nanoparticle GABA interactions: Complexation between the Keggin POM and γ-aminobutyric acid in the solid state and in solution influenced by additional ligands. *Inorg. Chim. Acta* **2021**, 526, 120547.
2. Dizaj, S.M.; Lotfipour, F.; Barzegar-Jalali, M.; Zarrintan, M.H.; Adibkia, K. Antimicrobial activity of the metals and metal oxide nanoparticles. *Mater. Sci. Eng. C* **2014**, 44, 278-284.
3. Almehizia, A.A.; Alkahtani, H.M.; Zen, A.A.; Obaidullah, A.J.; Naglah, A.M.; Alzughaibi, M.M.; Eldaroti, H.H. Complexes of the antibiotic drug succinylsulfathiazole with the La(III), Sm(III), and Tb(III) ions: Spectral characterizations, microscopic pictures, and thermal properties. *Bull. Chem. Soc. Ethiop.* **2025**, 39, 327-339.
4. Alsawat, M.; Adam, A.M.A.; Refat, M.S.; Alsuhaibani, A.M.; El-Sayed, M.Y. Structural, spectroscopic, and morphological characterizations of metal-based complexes derived from the reaction of 1-phenyl-2-thiourea with Sr^{2+}, Ba^{2+}, Cr^{3+}, and Fe^{3+} ions. *Bull. Chem. Soc. Ethiop.* **2024**, 38, 1803-1814.
5. Adam, A.M.A.; Refat, M.S.; Alsuhaibani, A.M.; El-Sayed, M.Y. Preparation and characterizations of metal-based complexes derived from the reaction of trizma base with Mg(II), Ca(II), and Ba(II) ions. *Bull. Chem. Soc. Ethiop.* **2024**, 38, 1791-1801.
6. El-Habeeb, A.A.; Refat, M.S. Synthesis, spectroscopic characterizations and biological studies on gold(III), ruthenium(III) and iridium(III) complexes of trimethoprim antibiotic drug. *Bull. Chem. Soc. Ethiop.* **2024**, 38, 701-714.
7. Alsuhaibani, A.M.; Adam, A.M.A.; Refat, M.S.; Kobeasy, M.I.; Bakare, S.B.; Bushara, E.S. Spectroscopic, thermal, and anticancer investigations of new cobalt(II) and nickel(II) triazine complexes. *Bull. Chem. Soc. Ethiop.* **2023**, 37, 1151-1162.
8. Eichhorn, G.L.; Marzilli, L.G. *Advances in Inorganic Biochemistry Models in Inorganic Chemistry*, PTR Prentice-Hall, Inc.: New Jersey; **1994**.
9. Hughes, M.N. *The Inorganic Chemistry of Biological Processes*, 2nd ed., Wiley: Chichester [England]; **1984**.

10. Mojos, K.D.; Orvig, C. Metallodrugs in medicinal inorganic chemistry. *Chem. Rev.* **2014**, 114, 4540-4563.
11. Alessio, E. *Bioinorganic Medicinal Chemistry*, Wiley-VCH Verlag GmbH and Co. KGaA: Germany; **2011**.
12. Younes, A.A.O.; Refat, M.S.; Saad, H.A.; Adam, A.M.A.; Alzoghibi, O.M.; Alsulaim, G.M.; Alsuhaibani, A.M. Complexation of some alkaline earth metals with bidentate uracil ligand: Synthesis, spectroscopic and antimicrobial analysis. *Bull. Chem. Soc. Ethiop.* **2023**, 37, 945-957.
13. Alkathiri, A.A.; Atta, A.A.; Refat, M.S.; Altalhi, T.A.; Shakya, S.; Alsawat, M.; Adam, A.M.A.; Mersal, G.A.M.; Hassanien, A.M. Preparation, spectroscopic, cyclic voltammetry and DFT/TD-DFT studies on fluorescein charge transfer complex for photonic applications. *Bull. Chem. Soc. Ethiop.* **2023**, 37, 515-532.
14. Adam, A.M.A.; Refat, M.S.; Gaber, A.; Grabchev, I. Complexation of alkaline earth metals Mg^{2+}, Ca^{2+}, Sr^{2+} and Ba^{2+} with adrenaline hormone: Synthesis, spectroscopic and antimicrobial analysis. *Bull. Chem. Soc. Ethiop.* **2023**, 37, 357-372.
15. Al-Hazmi, G.H.; Adam, A.M.A.; El-Desouky, M.G.; El-Bindary, A.A.; Alsuhaibani, A.M.; Refat, M.S. Efficient adsorption of Rhodamine B using a composite of Fe3O4@zif-8: Synthesis, characterization, modeling analysis, statistical physics and mechanism of interaction. *Bull. Chem. Soc. Ethiop.* **2023**, 37, 211-229.
16. Alsuhaibani, A.M.; Adam, A.M.A.; Refat, M.S. Four new tin(II), uranyl(II), vanadyl(II), and zirconyl(II) alloxan biomolecule complexes: synthesis, spectroscopic and thermal characterizations. *Bull. Chem. Soc. Ethiop.* **2022**, 36, 373-385.
17. Al-Hazmi, G.H.; Alibrahim, K.A.; Refat, M.S.; Ibrahim, O.B.; Adam, A.M.A.; Shakya, S. A new simple route for synthesis of cadmium(II), zinc(II), cobalt(II), and manganese(II) carbonates using urea as a cheap precursor and theoretical investigation. *Bull. Chem. Soc. Ethiop.* **2022**, 36, 363-372.
18. Alsuhaibani, A.M.; Refat, M.S.; Adam, A.M.A.; Kobeasy, M.I.; Kumar, D.N.; Shakya, S. Synthesis, spectroscopic characterizations and DFT studies on the metal complexes of azathioprine immunosuppressive drug. *Bull. Chem. Soc. Ethiop.* **2022**, 36, 73-84.
19. El-Sayed, M.Y.; Refat, M.S.; Altalhi, T.; Eldaroti, H.H.; Alam, K. Preparation, spectroscopic, thermal and molecular docking studies of covid-19 protease on the manganese(II), iron(III), chromium(III) and cobalt(II) creatinine complexes. *Bull. Chem. Soc. Ethiop.* **2021**, 35, 399-412.
20. Alosaimi, A.M.; Saad, H.A.; Al-Hazmi, G.H.; Refat, M.S. In situ acetonitrile/water mixed solvents: An ecofriendly synthesis and structure explanations of Cu(II), Co(II), and Ni(II) complexes of thioxoimidazolidine. *Bull. Chem. Soc. Ethiop.* **2021**, 35, 351-364.
21. Refat, M.S.; Altalhi, T.A.; Al-Hazmi, G.H.; Al-Humaidi, J.Y. Synthesis, characterization, thermal analysis and biological study of new thiophene derivative containing *o*-aminobenzoic acid ligand and its Mn(II), Cu(II) and Co(II) metal complexes. *Bull. Chem. Soc. Ethiop.* **2021**, 35, 129-140.
22. Barnhart, J. Occurrences, uses, and properties of chromium. *Regul. Toxicol. Pharmacol.* **1997**, 26, S3-S7.
23. Khilla, M.A.; Hanafi, Z.M.; Mohamed, A.K. Physico-chemical properties of chromium trioxide and its suboxides. *Thermochim. Acta* **1982**, 59, 139-147.
24. Kessi, A.; Delley, B. Density functional crystal vs. cluster models as applied to zeolites. *Int. J. Quantum Chem*. **1998**, 68, 135-144.
25. Delley, B. From molecules to solids with the $DMol^3$ approach. *J. Chem. Phys.* **2000**, 113, 7756-7764.
26. Hehre, W.J.; Radom, L.; Schleyer, P.R.; Pople, J.A. *Ab Initio Molecular Orbital Theory*, Wiley: New York; **1986**.

27. Ji, Z.; Santamaria, R.; Garzón, I.L. Vibrational circular dichroism and IR absorption spectra of amino acids: A density functional study. *J. Phys. Chem. A* **2010**, 114, 10, 3591-3601.
28. Mohamed, M.E.; Mohammed, A.M.A. Experimental and computational vibration study of amino acids. *Inter. Lett. Chem. Phys. Astro.* **2013**, 10, 1-17.
29. Han, J.; Chi, Y.S. Vibrational and electronic spectroscopic characterizations of amino acid-metal complexes. *J. Korean Soc. Appl. Biol. Chem.* **2010**, 53, 821-825.
30. Bellamy, L.J. *The infrared Spectra of Complex Molecules*, Chapman & Hall: London; **1975**.
31. Deacon, G.B.; Phillips, R.J. Relationships between the carbon-oxygen stretching frequencies of carboxylato complexes and the type of carboxylate coordination. *Coord. Chem. Rev.* **1980**, 33, 227-250.
32. Aljahdali, M.; El-Sherif, A.A. Synthesis, characterization, molecular modeling and biological activity of mixed ligand complexes of Cu(II), Ni(II) and Co(II) based on 1,10-phenanthroline and novel thiosemicarbazone. *Inorg. Chim. Acta* **2013**, 407, 58-68.